THE ASTROPHYSICAL JOURNAL, 334:626–638, 1988 November 15

OBSERVATIONAL AND THEORETICAL MASS-LOSS RATES OF O STARS IN THE MAGELLANIC CLOUDS

CLAUS LEITHERER[1]
Joint Institute for Laboratory Astrophysics, University of Colorado and National Bureau of Standards
Received 1988 February 22; accepted 1988 May 18

ABSTRACT

The stellar-wind properties of 26 luminous O stars in the Magellanic Clouds are investigated. Observational mass-loss rates are derived from the Hα emission in these stars. We find that mass-loss rates derived from Hα and from UV resonance lines agree if the velocity law and carbon- and nitrogen-ionization fractions of the wind are the same as in comparable galactic stars and if the canonical abundances for the Clouds are adopted. Theoretical mass-loss rates from the line-driven wind theory with line-force parameters appropriate for the Magellanic Clouds are computed. Theoretical and observational mass-loss rates disagree if the stellar parameters associated with a given spectral type are identical in the Galaxy and in the Magellanic Clouds. Due to the extreme sensitivity of a line-driven wind to the stellar luminosity, the mass-loss rates derived theoretically are strongly dependent on the adopted spectral-type/$T_{\rm eff}$ calibration. If the effective temperature of SMC stars is hotter by $\sim 10\%$ (and of LMC stars by $\sim 5\%$) than in galactic stars of identical spectral type, theoretical and observational mass-loss rates agree.

Subject headings: galaxies: Magellanic Clouds — stars: early-type — stars: mass loss

I. INTRODUCTION

Massive stellar winds are observed in galactic O stars, luminous B stars, and Wolf-Rayet stars (e.g., Lamers 1988). Numerical models for winds of O-type stars were first developed by Castor, Abbott, and Klein (1975, hereafter CAK). The basic idea is that the wind is initiated and maintained by transferring momentum to the flow by scattering of photospheric photons by spectral lines. In subsequent papers by Abbott (1982), Pauldrach, Puls, and Kudritzki (1986, hereafter PPK), Friend and Abbott (1986, hereafter FA), and Kudritzki, Pauldrach, and Puls (1987, hereafter KPP) the original theory has been improved significantly. Mass-loss rates ($\dot{M}$) predicted by the theory are in very good quantitative agreement with observed rates. The most reliable empirical mass-loss rates are derived from radio observations (e.g., Abbott 1985; Abbott *et al.* 1986).

Our current understanding of the evolution of massive stars has been profoundly influenced by the existence of mass loss in these stars (e.g., Chiosi and Maeder 1986). The evolutionary connection of objects such as O, Of, W-R stars, and luminous blue variables could be established after mass loss was incorporated in the evolutionary calculations. However, an important prediction of the CAK theory is the dependence of stellar-wind parameters on the chemical composition of the mass-losing star: stars with lower metal content should transfer less momentum to their winds. If this prediction holds, significant differences between the evolution of massive galactic and extragalactic stars might be expected.

This theoretical prediction is difficult to test on the basis of galactic O stars where metallicity differences are too small to produce a detectable effect. On the other hand, O stars in the Small and Large Magellanic Clouds (SMC and LMC) have metallicity differences of up to a factor of 10 relative to the Galaxy, so that the theory predicts significantly lower mass-loss rates and terminal velocities in these stars. Unfortunately, the distance of SMC/LMC stars excludes the most powerful tool to derive $\dot{M}$, i.e., radio observations, so that one is left with the UV and the Hα methods. A discussion of the various techniques to derive $\dot{M}$ can be found in Lamers (1988).

Bruhweiler, Parsons, and Wray (1982), Garmany and Conti (1985), Willis *et al.* (1986), Prinja (1987), and Garmany and Fitzpatrick (1988) investigated differences in stellar-wind properties between the Clouds and the Galaxy utilizing UV observations. Although generally lower wind velocities as predicted by the theory could be established, no conclusive evidence for an $\dot{M}$ difference could be found. This was partly ascribed to uncertainties in the adopted chemical abundances and the assumed ionization fractions, which affect the UV mass-loss rates. The alternative explanation could be that the prediction of the theory is not correct with respect to the metallicity dependence of $\dot{M}$.

Leitherer (1988, hereafter Paper I) has shown that Hα can be employed to derive mass-loss rates of galactic OB stars which are consistent with the values obtained by the UV- and radio method. Since Hα mass-loss rates are not affected by errors in the chemical composition and the ionization balance of the wind, this method can provide useful constraints on the dependence of $\dot{M}$ on the metallicity.

Hα observations of a sample of SMC/LMC stars are described in § II. Observational mass-loss rates are derived in § III. In § IV we compute mass-loss rates from the CAK theory and compare them with the observations. The influence of the adopted stellar parameters on the results is discussed in § V. Section VI compares Hα and UV mass-loss rates for SMC stars. Our conclusions are presented in § VII.

II. OBSERVATIONS AND DATA REDUCTION

Program stars were selected from the spectral classification work of Conti, Garmany, and Massey (1986), Garmany, Conti, and Massey (1987), and Garmany and Walborn (1987). These authors published a comprehensive catalog of two-

[1] Visiting Astronomer, Cerro Tololo Inter-American Observatory, National Optical Astronomy Observatories, which is operated by the Association of Universities for Research in Astronomy, Inc., under contract with the National Science Foundation.

TABLE 1A

STELLAR PARAMETERS AND OBSERVED MASS-LOSS RATES FOR PROGRAM STARS IN THE SMC

Star	Spectral Type	W_{obs} (Å)	S/N	M_v	log L ($L_\odot$)	T_{eff} (K)	log R ($R_\odot$)	M ($M_\odot$)	log g (cm s^{-2})	W_{net} (Å)	log L(Hα) ($L_\odot$)	$c(T_{eff})$	I	v_∞ (km s^{-1})	log $\dot{M}_{obs}$ ($M_\odot$ yr^{-1})
AV 14	O3–4 V	0.6e ± 0.9:	19	−5.6	5.98	50000	1.11	75	4.1	3.4:	0.53:	−6.71	1.21	2600	−5.58:
AV 15	O7 II	1.5a ± 0.6	21	−6.0	5.70	36000	1.26	40	3.5	0.8	0.06	−6.43	1.00	2000	−5.89
AV 26	O7 III	1.1a ± 0.4	24	−6.8	6.06	37000	1.41	50	3.3	1.2	0.56	−6.45	0.92	1500	−5.65
AV 39a	O4f	23e ± 5.8	10	−5.2	5.78	48000	1.05	60	4.1	26	1.26	−6.68	1.21	2600	−5.26
AV 69	O7 III	0.3a ± 0.6	21	−5.9	5.70	37000	1.23	40	3.6	2.1	0.44	−6.45	1.02	2100	−5.69
AV 70	O9.5 Iw	0.0 ± 0.5	22	−6.6	5.66	29000	1.43	35	3.1	1.7	0.63	−6.24	0.87	1300	−5.72
AV 75	O5 III	0.7a ± 0.4	29	−6.6	6.14	42500	1.33	75	3.7	1.8	0.66	−6.57	1.11	2500	−5.43
AV 232	O6.5 If	4.4e ± 0.4	21	−6.9	6.10	37500	1.42	55	3.3	6.7	1.35	−6.47	0.93	1600	−5.21
AV 243	O6 III	2.4a ± 0.4	15	−5.4	5.58	39500	1.12	35	3.7	0.2	−0.78	−6.51	1.08	2400	−6.29
AV 372	O9 I	0.6e ± 0.7	26	−6.7	5.86	32600	1.42	50	3.4	2.7	0.87	−6.34	0.93	1700	−5.48
AV 388	O4 V	1.9a ± 0.4	17	−5.2	5.78	48000	1.05	60	4.1	0.9	−0.21	−6.68	1.16	2600	−5.97
AV 398	O9.7 Ia	4.5e ± 2.0:	12	−6.2	5.46	28000	1.36	25	3.1	6.1:	1.03:	−6.20	0.84	1200	−5.60:
AV 411	O8.5 V	1.8a ± 0.3	16	−5.3	5.38	34000	1.15	30	3.6	0.5	−0.42	−6.38	0.97	2100	−6.17
AV 469	O8 II	1.6a ± 0.4	21	−6.0	5.66	34500	1.27	35	3.6	0.7	0.01	−6.39	0.97	1800	−5.96

TABLE 1B

STELLAR PARAMETERS AND OBSERVED MASS-LOSS RATES FOR PROGRAM STARS IN THE LMC

Star	Spectral Type	W_{obs} (Å)	S/N	M_v	log L ($L_\odot$)	T_{eff} (K)	log R ($R_\odot$)	M ($M_\odot$)	log g (cm s^{-2})	W_{net} (Å)	log L(Hα) ($L_\odot$)	$c(T_{eff})$	I	v_∞ (km s^{-1})	log $\dot{M}_{obs}$ ($M_\odot$ yr^{-1})
NS 5−67	O9.7 Ib	1.4e ± 0.2	24	−7.3	5.90	28000	1.58	50	3.0	3.0	1.16	−6.20	0.96	1300	−5.45
NS 22−65	O6 I	10e ± 0.7	17	−6.6	6.02	39000	1.35	45	3.4	12	1.50	−6.50	1.09	1700	−5.21
NS 69−67	O4 III(f)	0.2a ± 0.4	20	−6.0	6.02	45500	1.21	75	3.9	2.9	0.62	−6.63	1.30	2600	−5.56
NS 111−67	O7 f	1.5e ± 0.3	21	−6.0	5.74	37000	1.25	40	3.5	3.8	0.74	−6.45	1.18	2200	−5.60
NS 166−67	O4 I	3.9e ± 0.3	26	−6.3	6.10	44100	1.28	75	3.8	6.5	1.09	−6.61	1.27	2100	−5.38
NS 167−67	O4 Inf$^+$	4.0e ± 0.3	25	−6.4	6.14	44100	1.30	80	3.7	6.6	1.14	−6.61	1.27	2100	−5.35
NS 211−67	O3 III	2.9e ± 0.4	23	−6.2	6.22	50000	1.23	70	3.8	5.5	0.98	−6.71	1.25	3100	−5.24
NS 135−68	ON9.7 Ia	11e ± 0.5	25	−7.7	6.06	28000	1.66	55	2.9	12	1.93	−6.20	0.86	1100	−5.05
NS 137−68	O3 III(f*)	1.4e ± 0.5	22	−6.1	6.18	50000	1.21	65	3.8	4.0	0.80	−6.71	1.25	3100	−5.34
NS 189−66	O6.5 f	0.4e ± 0.7	13	−5.9	5.74	38000	1.23	40	3.6	2.9	0.58	−6.48	1.20	2300	−5.66
NS 266−67	O8:Iaf	13e ± 5.6:	22	−6.8	5.94	34200	1.42	50	3.3	15:	1.65:	−6.38	1.05	1700	−5.13:
NS 115−70	O4:III(f)	6.3e ± 0.4	19	−7.0	6.42	45500	1.41	100	3.6	8.7	1.50	−6.63	1.25	2600	−5.00

NOTE.—AV 39a = AB2 of Azzopardi and Breysacher 1979. This star has been classified O4f by Massey 1985.

dimensional MK spectral types for O stars in the LMC and SMC. Since the Hα method is most accurate if $\dot{M}$ is high (but Hα is still optically thin), we preferentially selected the most luminous O stars in the Clouds for the observing program. Contamination of the stellar Hα line by emission due to surrounding H II regions is much more serious for O stars in the Clouds than for O stars in the solar neighborhood. Therefore we excluded stars from our list which, from a visual inspection of photographic plates of the Clouds, were situated inside bright H II regions.

The final list of program stars actually observed comprises 12 stars in the LMC and 14 stars in the SMC. They are listed in Tables 1A (SMC) and 1B (LMC). The objects cover a typical magnitude range of $11.5 < V < 14.5$. The designation "AV" is from Azzopardi and Vigneau (1982) and "NS" from Sanduleak (1969), respectively.

All the spectra were obtained with the 1 m telescope at Cerro Tololo Inter-American Observatory (CTIO) during 10 nights in 1987 November. We used the 2D-Frutti Cassegrain spectrograph with a 600 lines mm^{-1} grating in second-order centered on Hα. The free spectral range was 2000 Å, and the spectral resolution as measured from emission lines after distortion correction and extraction of the spectrum was ~2.5 Å. The total exposure of an object was split into 2–4 individual exposures, with the star at different slit positions in order to optimize the flat-field correction. The slit covered ~4′ in the E-W direction of the sky. The long-slit capabilities of the 2D-Frutti were indispensable for the removal of nebular emission lines contaminating the stellar spectra (see below). Total exposure times ranged between 2–6 hr with typical signal-to-noise ratios of ~20. Since we did not intend to derive precise radial velocities, no effort has been made to obtain a large number of comparison spectra during the night. The HeAr comparison source was taken only at the beginning and at the end of the night.

Data reduction was performed using the NOAO/IRAF facilities installed at the VAX/8600 of the Joint Institute for Laboratory Astrophysics. Standard procedures as described in the 2D-Frutti Reduction Manual were applied. At first, the two-dimensional images were geometrically transformed to remove the strong image distortion. After dark subtraction, the star frames were flat-fielded using co-added dome and night-sky exposures. One-dimensional stellar spectra were obtained by using the "extraction" package of IRAF. This routine interactively determines and subtracts the background, traces the stellar spectrum perpendicular to the slit, and finally extracts

the spectrum with different weights according to the S/N of the individual CCD columns.

Hα equivalent widths of all program stars were measured in the wavelength-calibrated spectrograms. The error was estimated by testing different choices for the position of the continuum. Despite our effort to avoid stars with heavy contamination by Hα emission due to interstellar gas, ~30% of the objects showed nebular Hα emission on the two-dimensional CCD images, which was comparable or even stronger than the stellar continuum. In order to test the reliability of the background subtraction for the determination of the stellar Hα equivalent width, we chose a second, independent way to remove the nebular Hα. We measured the FWHM of the nebular line (which is unresolved and thus determined by the instrumental resolution) and subtracted a synthetic line profile of identical strength and FWHM from the (not background subtracted) stellar spectrum. Since the stellar photospheric absorption line and the wind emission are resolved and much broader than the nebular emission, the overlying nebular line is discernible as a sharp emission peak.

The two methods for measuring the stellar Hα equivalent width resulted in good agreement in nearly all cases. Tables 1A and 1B give the values measured for the equivalent widths together with the estimated errors (col. [3]). Column (4) of Tables 1A and 1B lists the signal-to-noise ratio as measured in the line-free continuum around Hα. Three values of W_{obs} are designated by a colon (:). AV 14 is situated in a region of strong and spatially extremely inhomogeneous nebular emission. Although W_{obs} as obtained by the two methods agree rather well (as reflected by the error given), the actual error may be higher. AV 398 and NS 266–67 are unique in that they show a very strong nebular Hα and [N II] emission contribution which is unresolved in the spatial as well as in the dispersion direction. The nebular Hα emission has been removed using the two nitrogen lines to measure the FWHM. These lines are emitted at a distance of less than ~0.5 pc from the star. As it is not clear if and how the nebular Hα emission is related to the stellar-wind Hα emission (which is present and much broader), we also consider the derived mass-loss rates uncertain. A discussion of the optical and ultraviolet spectra of NS 266–67 can be found in Walborn (1986) and Shore and Sanduleak (1984), respectively.

III. DERIVATION OF MASS-LOSS RATES

Mass-loss rates are derived in the same way as has been done for galactic stars in Paper I. We adopt the spectral types and the absolute visual magnitudes M_v published by Conti, Garmany, and Massey (1986), Garmany, Conti, and Massey (1987), and Garmany and Walborn (1987) (cols. [2] and [5] of Tables 1A and 1B). The absolute magnitudes are based on a distance modulus of 19.0 for the SMC and 18.3 for the LMC, respectively. A thorough discussion of the presently "best" values for the distance moduli of the Clouds is given by the above authors. In § V we shall discuss the influence of the distance on the derived $\dot{M}$ values.

Since the Hα method requires the effective temperature T_{eff} and the bolometric luminosity to derive $\dot{M}$, we have to assume a relation of these two parameters as a function of spectral type. This procedure is not trivial since a relation of this type has not yet been established for extragalactic O stars, and it is not necessarily obvious that the galactic relation can be applied without modification. In fact, the lower metal content Z of the Clouds may produce temperatures higher than in corresponding galactic stars due to changes in the opacity (see Brunish and Truran 1982). This affects the excitation and ionization conditions at the stellar surface which in turn are measured by spectral classification. Since the classification is done relative to galactic standards, we should expect that an O5 star of the SMC has the same excitation and ionization temperature at the stellar surface as a galactic O5 star. In principle, this effect, if observable, should lead to a proportionally higher fraction of earlier stars in the SMC and may thus influence the initial mass function but not the temperature scale. It is, however, not the excitation and ionization temperature which we are primarily interested in, but the effective temperature in order to derive radii R and bolometric luminosities L. Throughout §§ III and IV we shall assume that the relation between T_{eff} and the excitation and ionization temperature (i.e., spectral type) is not affected by metallicity differences. Hence we adopt Schmidt-Kaler's (1982*a*, *b*) spectral type/T_{eff} and spectral type/M_{bol} calibrations, which have been derived for galactic stars. The corresponding values for the program stars can be found in columns (6) (log L), (7) (T_{eff}), and (8) (log R) of Tables 1A and 1B. In § V we shall discuss the possibility of a different spectral type/T_{eff} relation and the consequences on the mass-loss determination.

Figure 1 shows the location of the program stars in the Hertzsprung-Russell diagram. We also plotted the theoretical main sequence and evolutionary tracks for galactic stars by Maeder and Meynet (1987). The program stars are situated in the uppermost part of the HRD, close to the observed upper limit (Humphreys 1987). Since no reliable evolutionary calculations for a grid of different values of $\dot{M}$ and Z have been published to date, we are forced to use the galactic tracks to obtain a mass estimate. All the program stars are still on the main sequence (by the definition of stellar evolution) where mass loss is not so crucially important as for post–main-sequence evolution so that we are confident that the estimated masses are accurate to within 50%. Such accuracy in $\dot{M}$ is entirely sufficient in deriving $\dot{M}$ from Hα. The stellar mass only enters when calculating a theoretical underlying photospheric absorption profile specified by T_{eff} and log g. A 50% error in M translates into an error of less than 0.2 in log g, which has negligible consequences for the equivalent width (see Auer and Mihalas 1972). Columns (9) and (10) of Tables 1A and 1B give the values derived for M and log g, respectively.

The observed Hα equivalent widths, which are supposed to be a superposition of a photospheric absorption profile and an optically thin wind emission, are corrected for the photospheric profile using non–LTE profiles published by Auer and Mihalas (1972). The resulting net equivalent width W_{net} can be found in column (11) of Tables 1A and 1B. The theoretical profiles have been calculated from model atmospheres with solar abundances. We do not expect a significant influence of Z on the photospheric Balmer-line equivalent widths. They depend on the equations of statistical equilibrium for the H atom which in turn are controlled by the run of the temperature. If the latter remains unchanged, the equivalent widths of the photospheric Balmer lines should not be significantly affected. This expectation is supported by spectra of SMC/LMC stars in the blue region. Although these stars show very faint metallic lines, the Balmer absorption lines have approximately the same strength as in corresponding galactic stars (C. D. Garmany, private communication).

The wind luminosities L(Hα) as obtained from W_{net} are summarized in column (12) of Tables 1A and 1B. As shown in

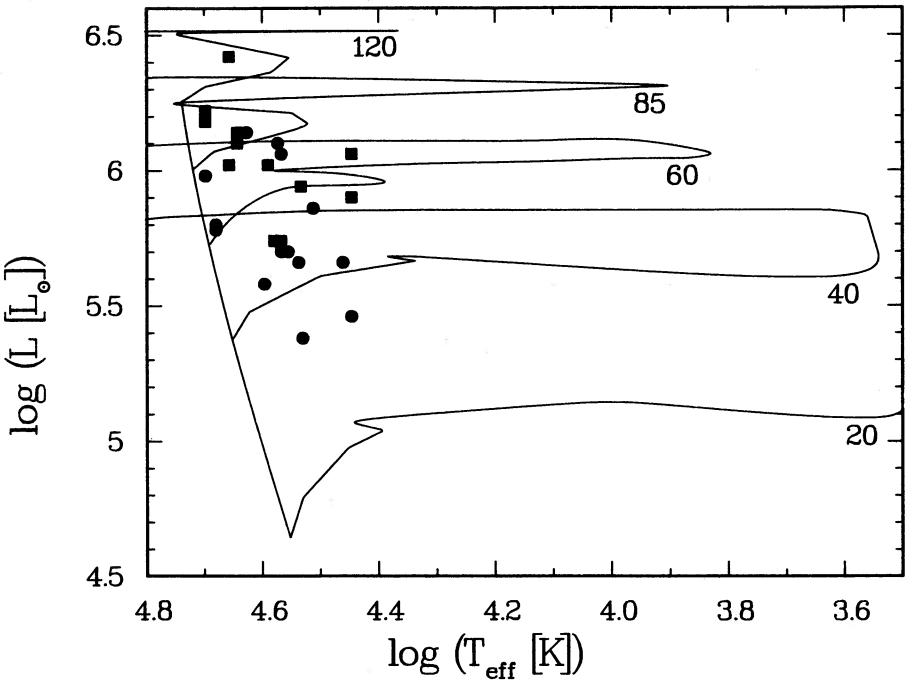

FIG. 1.—Hertzsprung-Russell diagram showing the location of the program stars (*filled circles*, SMC; *filled squares*, LMC). Evolutionary tracks for 120, 85, 60, 40, and 20 solar mass stars and the ZAMS are taken from Maeder and Meynet (1987).

Paper I, the stellar mass-loss rate is related to $L(\mathrm{H}\alpha)$ by

$$\log L(\mathrm{H}\alpha) = 2 \log |\dot{M}| - 2 \log v_\infty - \log R + c(T_{\mathrm{eff}}) + I + 25.125 , \quad (1)$$

where $L(\mathrm{H}\alpha)$ is in $L_\odot$, $\dot{M}$ is in $M_\odot$ yr^{-1}, v_∞ is in km s^{-1}, and R is in $R_\odot$. The quantity $c(T_{\mathrm{eff}})$ is a temperature-dependent factor introduced by the non–LTE–Saha equation. The quantity I is related to the velocity-law exponent β, which for LMC/SMC stars is $0.60 < \beta < 0.75$ (see § IV). The resulting values of $c(T_{\mathrm{eff}})$ and I are tabulated in columns (13) and (14) of Tables 1A and 1B, respectively. The adopted terminal velocities of the wind are in column (15) of Tables 1A and 1B. Section IV describes how v_∞ was obtained for each star. Finally, the mass-loss rates $\dot{M}_{\mathrm{obs}}$ computed via equation (1) are listed in the last column of Tables 1A and 1B.

In Figure 2 we show the dependence of the derived mass-loss rates on the luminosity. The error bars refer to the observational errors only. Obviously, $\dot{M}_{\mathrm{obs}}$ is well correlated with the stellar luminosity. For comparison, we plotted the galactic relation $\log \dot{M} = -6.87 + 1.62 \log (L/10^5)$ found by Garmany and Conti (1984). It should be emphasized that the galactic relation may only be compared to the SMC/LMC results if the stellar parameters are identical. Under this assumption we see from Figure 2 that the mass-loss rates in the Galaxy are not too much different from the rates in the Clouds. For a more quantitative approach to this question, however, we cannot simply use the statistical $\dot{M}$ formula as a comparison. Rather, one has to compute the theoretically predicted mass-loss rate for each star and compare it to the observations. This is described in the following section.

IV. MASS-LOSS RATES PREDICTED BY THE CAK THEORY

a) *Functional Dependence of $\dot{M}$ on Stellar and Wind Parameters*

Self-consistent wind models for a number of galactic O stars have been published, e.g., by PPK and FA, who performed several important improvements of the original CAK theory. Most importantly, they adopted a grid of realistic line opacities and did not make use of the finite-disk approximation. By accounting for the solid angle subtended by the stellar disk the radiation force is reduced close to the star and the theoretical $\dot{M}$ is lower than in the original CAK theory. The agreement of the improved theory with the observations is found to be very good. Clearly, comparing self-consistent wind models for Cloud stars to our observations would be the optimum way to test the theory. This is beyond the scope of the present paper.

PPK and FA found simple scaling relations to predict the theoretical mass-loss rate and the velocity law of the wind for an extensive grid of stellar parameters. We use their scaling relations to obtain the theoretical $\dot{M}$ which can be compared with the observations. FA find for the theoretical $\dot{M}$:

$$\dot{M} = \frac{2\pi GM}{\sigma_e v_{\mathrm{th}}} \alpha (1-\alpha)^{(1-\alpha)/\alpha} k^{1/\alpha} \Gamma^{1/\alpha} (1-\Gamma)^{-(1-\alpha)/\alpha} v_{\mathrm{esc}}^{-0.3} ; \quad (2)$$

v_{th} is the thermal velocity at the base of the wind, Γ is the ratio of radiative (in the continuum) over gravitational acceleration, and v_{esc} is the surface escape velocity. The properties of the stellar wind explicitly enter by the quantities k and α. The quantity k is related to the total number of accelerating lines, and α depends on the relative distribution of strong and weak lines. The basic assumption of equation (2) is that the line-force

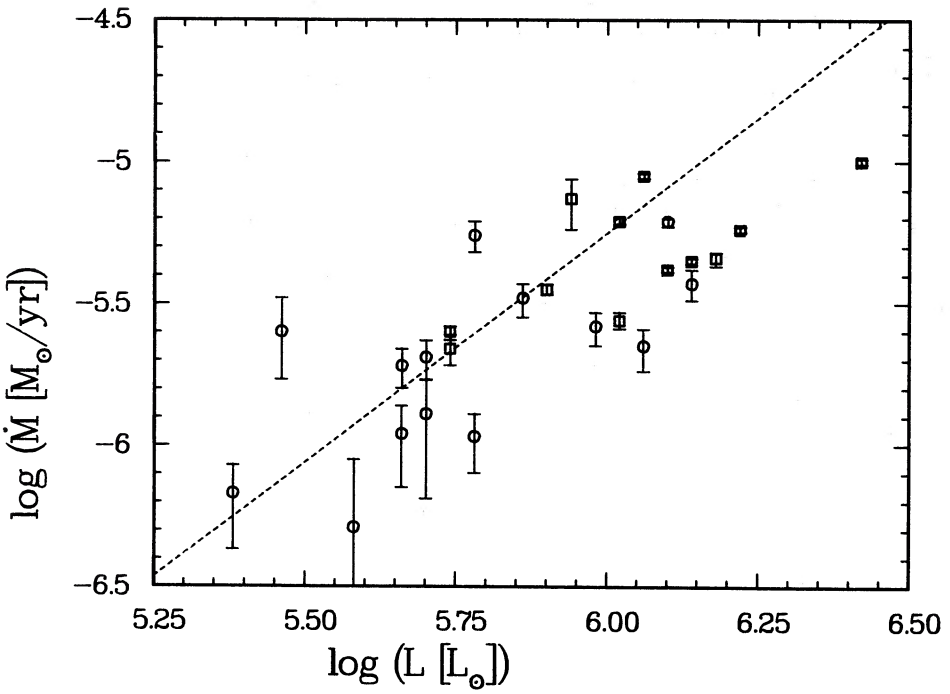

FIG. 2.—Observed mass-loss rates for stars in the SMC (*open circles*) and LMC (*open squares*) vs. luminosity. Dashed line is the relation for galactic stars found by Garmany and Conti (1984).

parameters α and k can be expressed in terms of some stellar parameters without the need to compute α and k self-consistently for every stellar model considered. KPP find that α and k can be well approximated by a functional dependence on $T_{\rm eff}$ and the metallicity Z. Their results, together with equation (2), can be used to predict the theoretical $\dot{M}$.

b) *Comparison of Theoretical and Observed $\dot{M}$ of Galactic O Stars Using an Empirical $v(r)$*

As a test of the reliability of these mass-loss rates, we computed the theoretical rates for all the galactic O stars with mass-loss rates derived from Hα in Paper I. After exclusion of O stars with upper limits for $\dot{M}$ this list comprises 71 stars. We find for the difference between the theoretical and the observed rates:

$$\log \dot{M}_{\rm CAK} - \log \dot{M}_{\rm obs} = -0.07 \pm 0.26 \,. \qquad (3)$$

Although there is a slight systematic difference in the sense that the observed rates are somewhat higher, the agreement is very satisfactory. The scatter and the slight systematic difference can be easily attributed to uncertainties in the distances, effective temperatures, etc. (see also the discussion in § V). Figure 3 shows the number distribution of the logarithmic differences binned in 0.05 intervals. The agreement between observed and theoretical rates implies that equation (2) together with the individual α and k values is very useful indeed to predict a theoretical $\dot{M}$ without the need to compute a self-consistent model in each case.

c) *Comparison of Theoretical and Observed $\dot{M}$ of Galactic O Stars Using the Theoretical $v(r)$*

The mass-loss rates used in equation (3) are based on the observationally derived velocity fields of the stellar winds. Since Hα luminosities measured for the stellar winds are sensitive to the wind density, a velocity field has to be assumed to derive $\dot{M}$. The radiation-pressure–driven wind theory also predicts velocity-law parameters β and v_∞ in terms of the stellar parameters and the line-force parameters α, k, and δ (δ accounts for variations of the ionization balance in the stellar wind). The velocity law is related to β and v_∞ in the usual way:

$$v(r) = v_\infty \left(1 - \frac{R}{r}\right)^\beta . \qquad (4)$$

In contrast to the results for the mass-loss rate, it is not possible to give a simply analytical relation for β and v_∞ which holds for all types of O stars. While the results of PPK and FA agree in a prediction of $\beta \approx 0.8$ for galactic stars, their scaling relations given systematically different values for the terminal velocities. Figure 4 compares the scaling relations of FA (their eq. [8]) and PPK (their eq. [35]) with the values actually observed for v_∞. The theoretical values use $\alpha = 0.6$, $\delta = 0.075$, and $R_c = 1.036$. We emphasize that a variation in $v_{\rm esc}$ also corresponds to a variation in $T_{\rm eff}$ and thus also in α, so that the entire observed range of $v_\infty/v_{\rm esc}$ cannot be accounted for by one value of α. Adopting the correct value of α in a self-consistent model generally leads to very good agreement between theory and observations. It is evident, however, from Figure 4 that for a typical value of α the two scaling relations systematically disagree. Note that this refers only to the scaling relations but not to the actual self-consistent models (D. C. Abbott, private communication). We find that FA's parameterization generally gives better results for O supergiants, whereas PPK's relation is the better choice for O dwarf stars if α is around 0.6. Therefore, somewhat arbitrarily, we adopt FA's equation (8) if $v_{\rm esc} < 900$ km s^{-1} and PPK's equation (35) if $v_{\rm esc} \geq 900$ km s^{-1} to predict v_∞. Throughout this paper we adopt this criterion when calculating theoretical terminal velocities, and we use PPK's equation (34) when calculating values for β. Since the maximum difference between both relations is

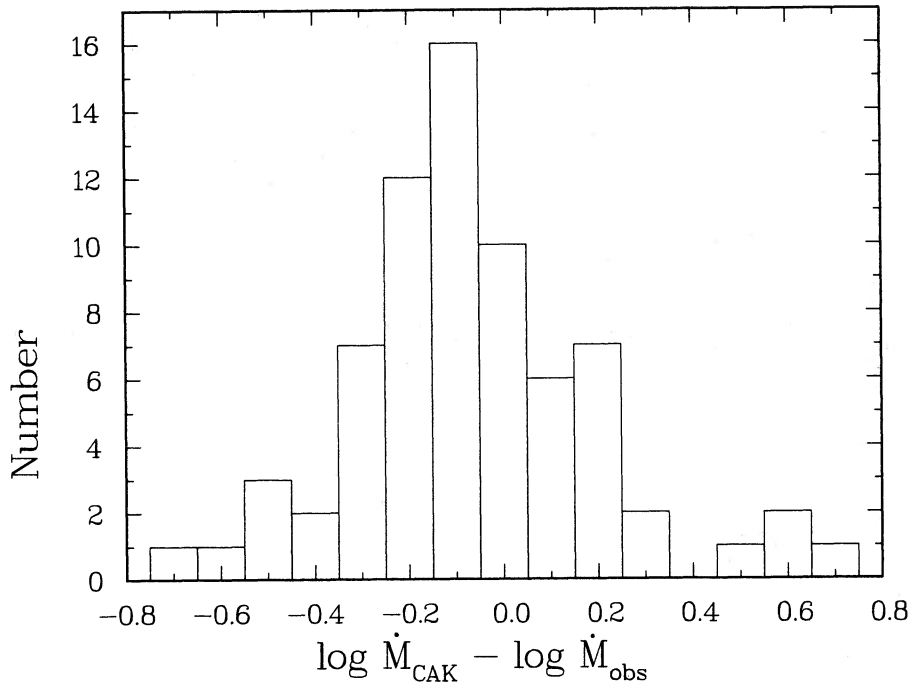

FIG. 3.—Histogram showing the residuals of the theoretical mass-loss rates ($\dot{M}_{CAK}$) and the rates derived for galactic stars in Paper I ($\dot{M}_{obs}$)

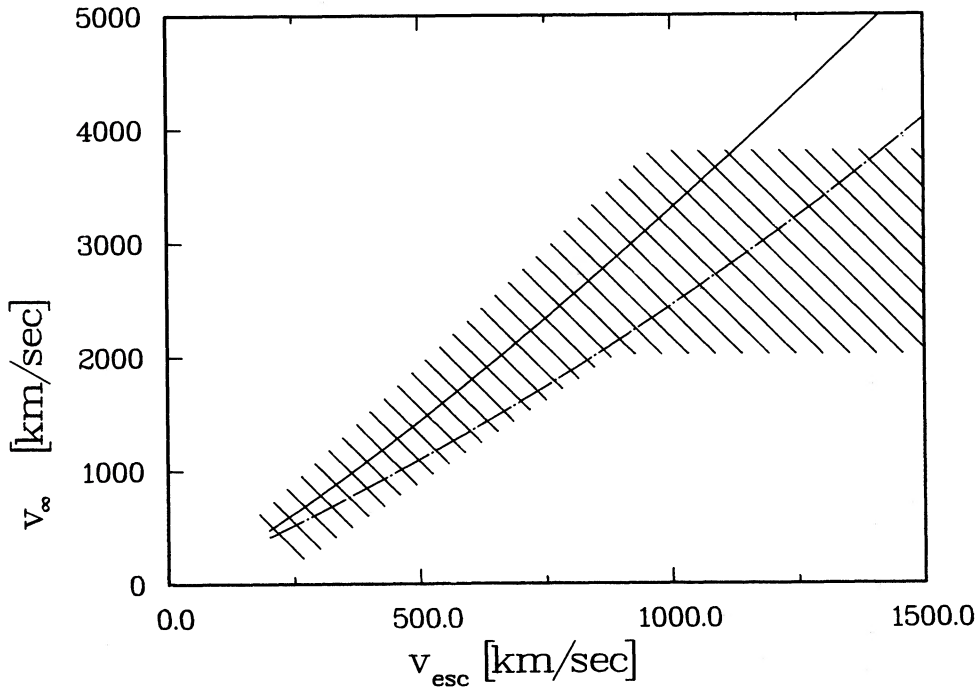

FIG. 4.—Plot of the terminal velocity vs. surface escape velocity. Shaded area roughly outlines the observed values. Solid line is FA's parameterization; dashed-dotted line is from PPK ($\alpha = 0.6$, $\delta = 0.075$, $R_c = 1.036$).

typically less than ~30% for v_∞, the influence on the derivation of $\dot{M}$ from the theoretical v_∞ is comparatively weak.

As a test of the consistency of the theoretical scaling relations for $\dot{M}$ and $v(r)$ we recalculated the empirical mass-loss rates of Paper I using the predicted values of v_∞ and β for each star. In this case one finds

$$\log \dot{M}_{\rm CAK} - \log \dot{M}_{\rm obs} = -0.05 \pm 0.25 \,. \quad (5)$$

Figure 5 is the counterpart of Figure 3, but with the results of equation (5). No significant differences between these methods can be found. This is a very encouraging result, implying that the predictions of the wind theory are in good agreement with mass-loss rates obtained from Hα even if the velocity law is adopted from the theory.

d) Application to Magellanic Cloud Stars

We apply the scaling relations discussed above to our sample of SMC/LMC stars to predict theoretical mass-loss rates and velocity laws. Since the majority of the program stars lacks observational determinations of v_∞ and β, we adopted theoretical velocity laws to derive the observed values of $\dot{M}$ from equation (1). The results found in the case of the galactic O stars justify this procedure. For consistency, we will also keep to the theoretical terminal velocities even in those cases where v_∞ has been measured by UV observations.

The numerical values for the line-force parameters α, δ, and k are interpolated from the tables published by KPP. Tables 2A and 2B summarize the relevant data for the SMC and the LMC, respectively: the line-force parameters (cols. [2], [3], [4]) based on $Z(\mathrm{SMC}) = 0.1Z(\mathrm{MW})$ and $Z(\mathrm{LMC}) = 0.28Z(\mathrm{MW})$, Γ (col. 5), the surface escape velocity corrected for continuum radiation pressure (col. 6), the velocity-law exponent β (col. 7), the terminal velocity (col. 8), and the theoretical mass-loss rate (col. 9). Notice that v_∞ in column (8) of Tables 2A and 2B is identical with the entries for v_∞ in Tables 1A and 1B, i.e., we used the theoretical values of v_∞ (and also of β) to derive the observational $\dot{M}$ from equation (1).

As expected, the theoretical $\dot{M}$ values are lower if compared with stars having the same stellar parameters but solar abundances. We did the same calculation of Table 2 but adopted KPP's line-force parameters for galactic abundances. The differences in log $\dot{M}$ between the two sets of calculations are

$$\log \dot{M}[Z(\mathrm{SMC})] - \log \dot{M}[Z(\mathrm{MW})] = -0.44 \pm 0.05 \,, \quad (6)$$

$$\log \dot{M}[Z(\mathrm{LMC})] - \log \dot{M}[Z(\mathrm{MW})] = -0.23 \pm 0.07 \quad (7)$$

where $\dot{M}[Z(\mathrm{SMC})]$ and $\dot{M}[Z(\mathrm{LMC})]$ refer to the entries in Tables 2A and 2B, respectively, and $\dot{M}[Z(\mathrm{MW})]$ refers to the calculations for the SMC/LMC stars assuming galactic abundances. KPP give an average functional dependence of log $\dot{M} \sim 0.47 \log Z$ for a typical O5 V star; i.e., one would expect values of -0.47 and -0.26 for the right-hand sides of equations (6) and (7), respectively. While our mean results are close to this functional dependence, we find significant departures for late-O supergiants. The radiation-pressure theory predicts a lower influence of metallicity on $\dot{M}$ in late-O stars than in hotter stars. (The most extreme example is NS 135−68 where the metallicity difference between the Galaxy and the LMC results in a log $\dot{M}$ difference of only -0.09.)

Figure 6 compares the observed and the theoretical rates of the program stars. The theoretical values use the line-force parameters for SMC and LMC abundances, respectively. The observed mass-loss rates are systematically higher than the rates predicted by the radiation-pressure–driven wind theory. We find for the mean difference between theory and observations:

$$\log \dot{M}_{\rm the} - \log \dot{M}_{\rm obs} = -0.38 \pm 0.29 \quad (\mathrm{SMC}) \,, \quad (8)$$

$$\log \dot{M}_{\rm the} - \log \dot{M}_{\rm obs} = -0.15 \pm 0.14 \quad (\mathrm{LMC}) \,. \quad (9)$$

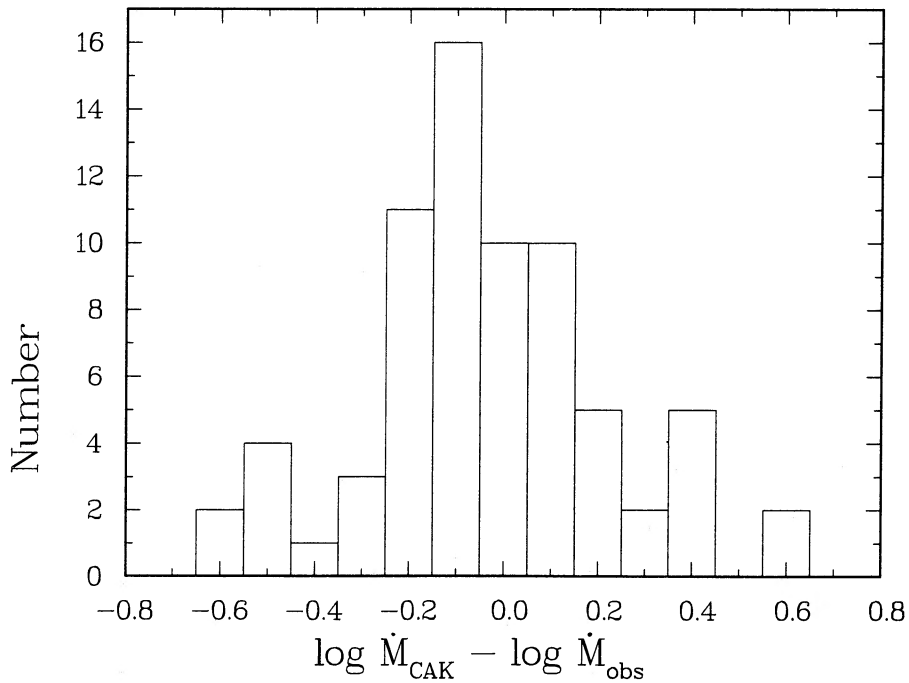

FIG. 5.—Same as Fig. 3, but for observed mass-loss rates recalculated with the theoretical velocity law

TABLE 2A

THEORETICAL MASS-LOSS RATES FOR SMC STARS

Star	α	δ	k	Γ	v_{esc} (km s^{-1})	β	v_∞ (km s^{-1})	log $\dot{M}_{the}$ ($M_\odot$ yr^{-1})
AV 14	0.583	0.100	0.096	0.29	1300	0.71	2600	−6.04
AV 15	0.554	0.136	0.114	0.29	770	0.63	2000	−6.20
AV 26	0.556	0.134	0.112	0.53	590	0.63	1500	−5.46
AV 39a	0.580	0.101	0.096	0.23	1300	0.71	2600	−6.34
AV 69	0.556	0.134	0.112	0.29	800	0.64	2100	−6.21
AV 70	0.534	0.147	0.150	0.30	590	0.60	1300	−6.03
AV 75	0.572	0.113	0.100	0.42	880	0.67	2500	−5.64
AV 232	0.559	0.132	0.110	0.52	620	0.63	1600	−5.46
AV 243	0.565	0.125	0.106	0.25	870	0.66	2400	−6.42
AV 372	0.545	0.142	0.128	0.33	700	0.62	1700	−5.90
AV 388	0.580	0.101	0.096	0.23	1300	0.71	2600	−6.34
AV 398	0.531	0.148	0.160	0.26	560	0.59	1200	−6.27
AV 411	0.548	0.140	0.121	0.18	820	0.63	2100	−6.74
AV 469	0.550	0.139	0.119	0.30	710	0.63	1800	−6.19

TABLE 2B

THEORETICAL MASS-LOSS RATES FOR LMC STARS

Star	α	δ	k	Γ	v_{esc} (km s^{-1})	β	v_∞ (km s^{-1})	log $\dot{M}_{the}$ ($M_\odot$ yr^{-1})
NS 5−67	0.545	0.110	0.196	0.36	570	0.63	1300	−5.42
NS 22−65	0.584	0.073	0.120	0.53	600	0.70	1700	−5.36
NS 69−67	0.618	0.089	0.094	0.32	1100	0.75	2600	−5.76
NS 111−67	0.575	0.076	0.132	0.31	770	0.70	2200	−5.92
NS 166−67	0.611	0.078	0.100	0.38	970	0.74	2100	−5.58
NS 167−67	0.611	0.078	0.100	0.40	960	0.74	2100	−5.50
NS 211−67	0.630	0.103	0.088	0.54	850	0.73	3100	−5.31
NS 135−68	0.545	0.110	0.196	0.48	490	0.62	1100	−5.05
NS 137−68	0.630	0.103	0.088	0.53	850	0.73	3100	−5.35
NS 189−66	0.579	0.074	0.125	0.31	790	0.71	2300	−5.95
NS 266−67	0.563	0.087	0.148	0.40	660	0.67	1700	−5.52
NS 115−70	0.618	0.089	0.094	0.60	770	0.73	2600	−5.00

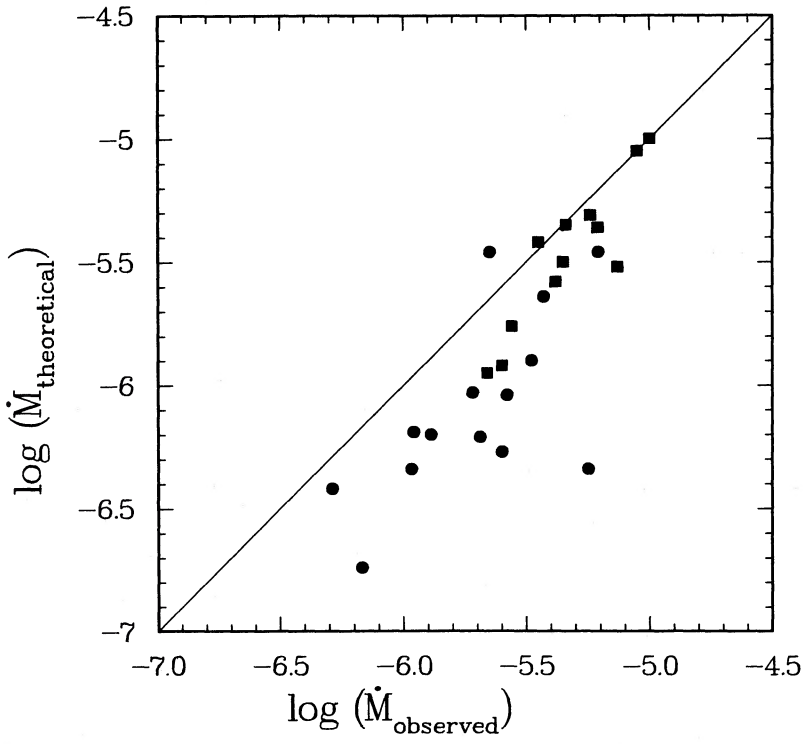

FIG. 6.—Theoretical vs. observed mass-loss rates for stars in the SMC (*filled circles*) and LMC (*filled squares*)

These results are virtually unaffected by the adopted theoretical terminal velocities. Ten out of 14 SMC program stars have published values of v_∞ (Prinja 1987; Garmany and Fitzpatrick 1988). Using these terminal velocities instead of the theoretical ones leads to a value of -0.39 ± 0.27 for the right-hand side of equation (8).

In contrast to the results found for the solar neighborhood, theoretical and observed mass-loss rates do not agree if the stars have a chemical composition different from the Sun. The observed rates are comparable to what is found in galactic stars of the same spectral type (see also Fig. 2). On the other hand, the theoretical values for $\dot{M}$ in the Clouds are lower by a factor of about $\sim(Z)^{1/2}$ producing the disagreement visible in Figure 6. This conclusion, however, rests on the assumption that stellar parameters of stars having identical spectral types are exactly the same in the Galaxy and in the Magellanic Clouds. In the following section we study the influence of varying certain stellar parameters on the resulting mass-loss rates.

V. INFLUENCE OF THE ADOPTED STELLAR PARAMETERS

The derived observed and theoretical mass-loss rates are obviously sensitive to the adopted stellar parameters. Basically, these parameters are extracted from the spectral classification, which gives the effective temperature and the bolometric correction, and the distance moduli of the Clouds, from which the absolute visual magnitudes are derived.

The distance moduli of the Clouds are not very well established. In order to illustrate the influence of the distance on the derived mass-loss rates, we scaled the previously adopted distances to the Clouds by 10%, i.e., we make the assumption the SMC distance modulus is 19.2 and that of the LMC is 18.5, respectively. Such scaling is surely within the errors for the distance moduli. The new distances affect $\dot{M}_{\rm obs}$ as well as $\dot{M}_{\rm the}$.

We recalculated all the steps of §§ III and IV with the new distance moduli. The new mass-loss rates are summarized in columns (2) and (3) of Tables 3A and 3B for the SMC and LMC, respectively. Both the observed as well as the theoretical rates are higher now. The influence of the distance d on the observed rates is comparatively small, the mean increase of all 26 stars is 0.05 in $\log \dot{M}_{\rm obs}$. The influence on the theoretical rates is higher; we find an average increase by 0.14. These results can easily be understood from equations (1) and (2).

The observationally derived mass-loss rates scale with the distance as $\dot{M} \sim d^{3/2}$ due to the distance dependence of R and $L(\mathrm{H}\alpha)$. Since we used the theoretical velocity laws, which are also dependent on the assumed distance, the functional dependence of $\dot{M}$ on d will be slightly modified. This effect, however, is hardly noticeable in the scaled $\dot{M}_{\rm obs}$.

The influence of the distance on theoretical mass-loss rates enters via the mass, Γ (i.e., the luminosity and mass), and the surface escape velocity in equation (2). Assuming a mass-luminosity relation of $L \sim M^2$, one finds $M \sim d$, and, since $\Gamma \sim L/M$, we have $\Gamma \sim d$. A further dependence on d is introduced by the factor $(1-\Gamma)^{-(1-\alpha)/\alpha}$ in equation (2) and by $v_{\rm esc}$ which provides an additional factor $(1-\Gamma)^{-0.15}$. This latter factor, however, can be neglected for a rough estimate unless $\Gamma \approx 1$. Combining the above factors leads to:

$$\dot{M}_{\rm the} \sim d^{1+1/\alpha}(1-\Gamma)^{-(1-\alpha)/\alpha} . \quad (10)$$

For typical values of Γ and α, the second factor in equation (10) makes only a 10%–20% correction (toward higher mass-loss rates) to the distance dependence of the first factor. Inserting a distance increase by 10%, these scaling relations predict to a good approximation the mass-loss rates actually derived.

TABLE 3A

OBSERVED AND THEORETICAL MASS-LOSS RATES FOR SCALED DISTANCES AND EFFECTIVE TEMPERATURES: SMC STARS

Star	$\log \dot{M}_{\rm obs}$ (d')	$\log \dot{M}_{\rm the}$ (d')	$\log \dot{M}_{\rm obs}$ ($T'_{\rm eff}$)	$\log \dot{M}_{\rm the}$ ($T'_{\rm eff}$)
AV 14	−5.53	−5.91	−5.57	−5.71
AV 15	−5.83	−6.09	−5.87	−5.85
AV 26	−5.59	−5.33	−5.71	−4.90
AV 39a	−5.21	−6.23	−5.24	−6.00
AV 69	−5.64	−6.11	−5.67	−5.84
AV 70	−5.68	−5.90	−5.70	−5.68
AV 75	−5.39	−5.50	−5.45	−5.21
AV 232	−5.19	−5.28	−5.30	−4.93
AV 243	−6.25	−6.28	−6.29	−6.09
AV 372	−5.43	−5.77	−5.48	−5.57
AV 388	−5.92	−6.23	−5.98	−6.00
AV 398	−5.55	−6.12	−5.58	−5.94
AV 411	−6.12	−6.60	−6.15	−6.40
AV 469	−5.90	−6.06	−5.94	−5.87

TABLE 3B

OBSERVED AND THEORETICAL MASS-LOSS RATES FOR SCALED DISTANCES AND EFFECTIVE TEMPERATURES: LMC STARS

Star	$\log \dot{M}_{\rm obs}$ (d')	$\log \dot{M}_{\rm the}$ (d')	$\log \dot{M}_{\rm obs}$ ($T'_{\rm eff}$)	$\log \dot{M}_{\rm the}$ ($T'_{\rm eff}$)
NS 5−67	−5.40	−5.26	−5.45	−5.23
NS 22−65	−5.19	−5.19	−5.25	−5.12
NS 69−67	−5.51	−5.64	−5.58	−5.61
NS 111−67	−5.55	−5.80	−5.60	−5.78
NS 166−67	−5.34	−5.44	−5.35	−5.41
NS 167−67	−5.30	−5.39	−5.14	−5.34
NS 211−67	−5.21	−5.17	−5.27	−5.11
NS 135−68	−5.02	−4.89	−5.06	−4.85
NS 137−68	−5.32	−5.20	−5.36	−5.16
NS 189−66	−5.61	−5.83	−5.68	−5.79
NS 266−67	−5.08	−5.37	−5.14	−5.35
NS 115−70	−4.98	−4.84	−5.02	−4.77

The larger distance moduli result in better agreement between theoretical and observed rates. The mean differences of $\log \dot{M}$ are now

$$\log \dot{M}_{\rm the} - \log \dot{M}_{\rm obs} = -0.30 \pm 0.30 \quad (\mathrm{SMC}) , \quad (11)$$

$$\log \dot{M}_{\rm the} - \log \dot{M}_{\rm obs} = -0.04 \pm 0.16 \quad (\mathrm{LMC}) . \quad (12)$$

The $\dot{M}_{\rm obs}$ and $\dot{M}_{\rm the}$ of the LMC are virtually in agreement, but for the SMC even a change by 0.2 in the distance modulus was not sufficient to reconcile theory and observations. This can be appreciated from Figure 7 which illustrates the influence of d on both the observed and the theoretical rates. The observed SMC rates are still significantly higher than the theoretical ones. Formally, agreement could be enforced if the distance modulus of the SMC were approximately $d \approx 20.2$.

The second basic stellar parameter which may be subject to a systematic error is the effective temperature. As already outlined in § III, the derived mass-loss rates rest on the assumption of equal $T_{\rm eff}$ scales in the solar neighborhood and the Magellanic Clouds. We can test the influence of the temperature scale on $\dot{M}$ by (arbitrarily) assuming $T_{\rm eff}$ of all O subtypes in the SMC to be 10% higher than in corresponding galactic stars. For the LMC we adopt a difference of 5% only. Furthermore, we assume that the bolometric correction scale

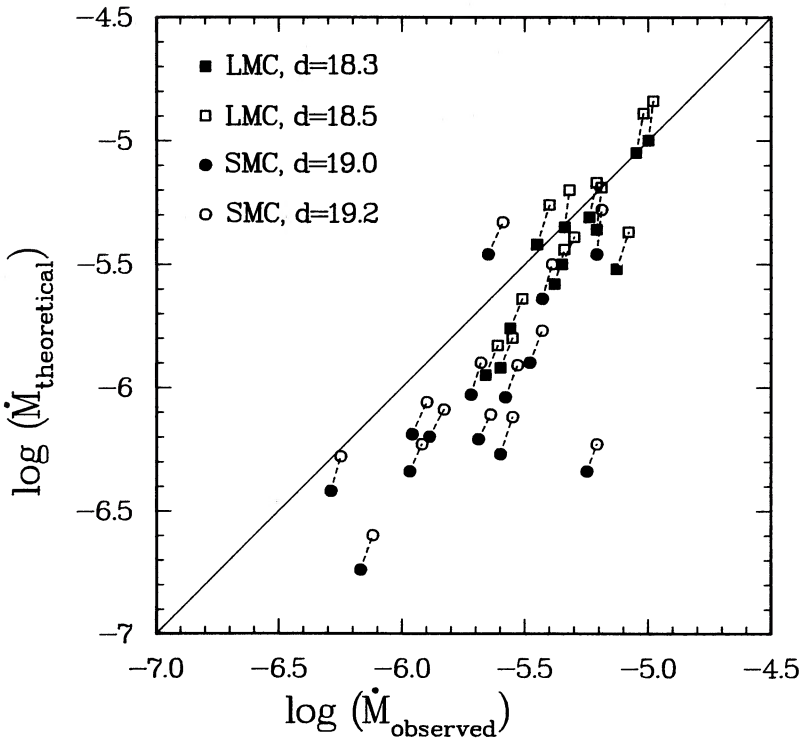

FIG. 7.—Diagram illustrating the influence of the assumed distance of the Clouds on the derived observed and theoretical mass-loss rates

changes correspondingly; i.e., the stellar radius is kept constant.

Again we can go through all the steps of §§ III and IV to find the new mass-loss rates listed in columns (4) and (5) of Tables 3A and 3B. The observed values are unaffected by a hotter temperature scale. The mean difference between the logarithms of the old and the new observed mass-loss rates is 0.00. On the other hand, the theoretical values are increased dramatically. In the LMC the mean difference caused by the hotter $T_{\rm eff}$ scale amounts to 0.18, in the SMC, we find a difference of 0.38.

The behavior of the observed rates is easily explainable by the temperature dependence of equation (1). The quantity $T_{\rm eff}$ only enters via the Saha factor $c(T_{\rm eff})$ which varies rather slowly if $T_{\rm eff} > 30{,}000$ K (see Paper I). As in the case above, we also have a weak indirect influence by the velocity law (including v_∞), which is calculated theoretically. (In fact, the large $\dot{M}_{\rm obs}$ difference for NS 167−67 is exclusively due to a difference in v_∞. Our relation for v_∞ as a function of $v_{\rm esc}$ is discontinuous at $v_{\rm esc} = 900$ km s^{-1}, as explained in § IV. Since $v_{\rm esc}$ of this star happens to shift from 960 to 890 km s^{-1} due to the hotter $T_{\rm eff}$ scale, v_∞ also shows this discontinuity.)

The extreme sensitivity of the theoretical rates is primarily due to the strong luminosity dependence of a radiation-pressure driven wind. The dominant luminosity dependence in equation (2) is the $\Gamma^{1/\alpha}$ factor, which for $\alpha = 0.56$ implies $\dot{M} \sim L^{1.79}$. Since to a good approximation $L \sim T_{\rm eff}^4$, the theoretical mass-loss rate scales with $T_{\rm eff}$ with a power of ~ 7! Thus an increase of $T_{\rm eff}$ by 10% leads to an increase in $\log \dot{M}_{\rm the}$ by ~ 0.3 in the SMC. The actual value is even higher by about a factor of 1.2 due to the combined effect of the remaining factors in equation (2). The terminal velocities of the wind are much less affected by the temperature scale. They are determined by $v_{\rm esc}$ and the line-force parameters, which produce a decrease of v_∞ by 10%–20%.

We note that the stellar mass has been assumed to be unaffected by a scaling of the temperature. If the temperature scale is different in the Clouds, the theoretical mass-luminosity relation may also be different. Since we do not know if and how the M-L relation changes, M had not been scaled for simplicity. This, however, has only minor consequences for the theoretical $\dot{M}$.

Adopting the new temperature scales (10% and 5% higher for SMC and LMC, respectively) results in good agreement between observed and theoretical mass-loss rates in both Clouds. The mean differences are

$$\log \dot{M}_{\rm the} - \log \dot{M}_{\rm obs} = -0.01 \pm 0.36 \quad \text{(SMC)}, \qquad (13)$$

$$\log \dot{M}_{\rm the} - \log \dot{M}_{\rm obs} = +0.02 \pm 0.19 \quad \text{(LMC)}. \qquad (14)$$

Figure 8 shows the influence of the two temperature scales on the derived mass-loss rates. No attempt has been made to optimize the agreement between theory and observations. The scaling factors of 1.05 and 1.10 have been chosen to yield approximate agreement and to illustrate the strong sensitivity of the theoretical rates for the temperature scale. We emphasize that a higher $T_{\rm eff}$ scale for the Clouds is an ad hoc assumption with only very weak (if at all) observational evidence. On the other hand, this assumption is not entirely implausible. Abbott and Hummer (1985) investigated the effect of back scattering by stellar winds on the temperature structure of the underlying stellar photosphere. They find a dependence of the effective temperature as derived from the spectral type on the stellar mass-loss rate: lower mass-loss rates are associated with comparatively higher effective temperatures for a given spectral type. In principle, this is consistent with the situation in the Clouds where a lower Z should give reduced photospheric and stellar wind blanketing. Fine analyses of O-star atmospheres in the Clouds with line-blanketed model atmospheres are necessary to support or reject this scenario.

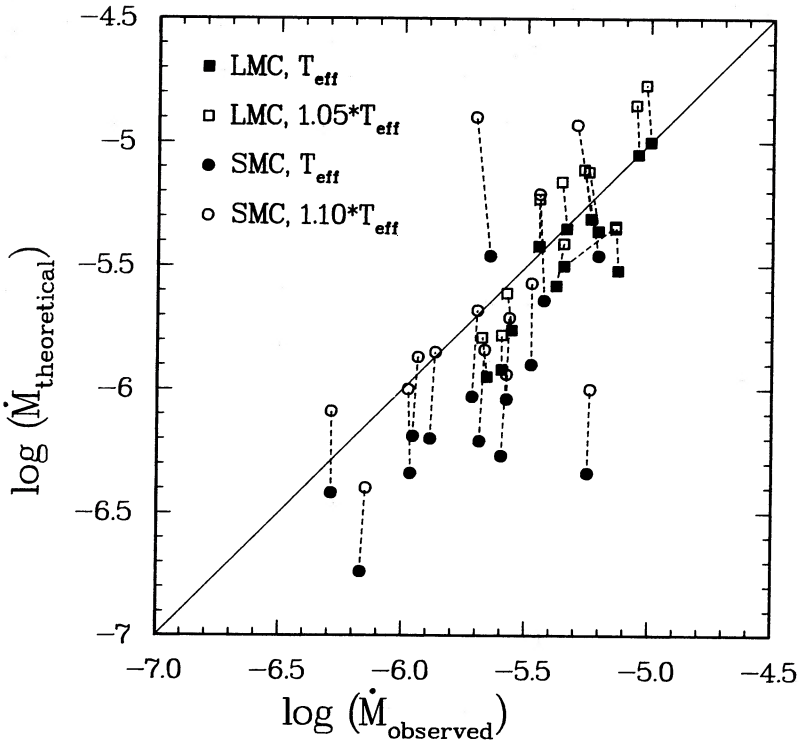

FIG. 8.—Same type of diagram as Fig. 8, but illustrating the influence of the T_{eff} scale

VI. COMPARISON WITH UV MASS-LOSS RATES

Ten program stars in the SMC have also been investigated in the UV to derive mass-loss rates (Prinja 1987; Garmany and Fitzpatrick 1988). As outlined in the Introduction, the derivation of $\dot{M}$ in the Magellanic Clouds from UV data is severely hampered by the insufficient knowledge of the chemical abundances and the ionization fractions (q_i) in the stellar winds. On the other hand, a comparison of mass-loss rates derived from Hα and from the UV can provide important constraints on these quantities since Hα is unaffected by uncertainties in Z and q_i.

We adopt the observed mass-loss rates of Tables 1A and 1B (i.e., based on the unscaled distances and effective temperatures) for the comparison with the UV. Table 4 lists the 10 program stars in common with the two above UV sources. The UV data were scaled to account for differences in the adopted radii and the terminal velocities for the derivation of $\dot{M}$. In addition, Prinja's data were reduced to an assumed SMC abundance of 0.1 the galactic value. A comparison of the scaled $\dot{M}q_i$ values and the Hα mass-loss rates then yields the empirical ionization fractions for C^{3+} and N^{4+} tabulated in columns (3) and (4) of Table 4. No significant correlation of the ionization fractions with T_{eff} or other stellar parameters can be found. The mean values are

$$\log q_i(\text{C IV}) = -2.0 \pm 0.3\,, \quad \text{(SMC)} \tag{15}$$

$$\log q_i(\text{N V}) = -1.4 \pm 0.3\,. \tag{16}$$

TABLE 4

IONIZATION FRACTIONS FOR C IV AND N V

Star	Source for UV	log q_i(C IV)	log q_i(N V)
AV 15	1	−2.0	−1.3
AV 26	2	−2.4	−1.7
AV 69	1	−2.1	...
AV 70	2	−2.3	−1.8
AV 75	1	−2.0	−1.3
AV 243	1	−1.8	−1.3
AV 243	2	−1.7	−0.9
AV 388	1	−2.2	−1.0
AV 398	2	−2.1	...
AV 411	1	−2.4	−1.9
AV 469	2	−1.4	−1.1

SOURCES.—(1) Garmany and Fitzpatrick 1988; (2) Prinja 1987.

The ionization fractions derived for the SMC can be compared with the corresponding values found for galactic O stars. Garmany *et al.* (1981) obtained high-resolution *IUE* spectra of a representative sample of galactic O stars. Fourteen program stars of their sample showed unsaturated C IV and/or N V profiles, which allow us to derive mass-loss rates and ionization fractions. Since Garmany *et al.* did not list q_i for their program stars, we used their equations (8a) and (8b) to derive these quantities. The mean values for the galactic stars are

$$\log q_i(\text{C IV}) = -2.1 \pm 0.2\,, \quad \text{(Galaxy)} \tag{17}$$

$$\log q_i(\text{N V}) = -1.5 \pm 0.2\,. \tag{18}$$

Given the uncertainties and the scatter, we conclude that there is no significant difference in the ionization fractions of C^{3+} and N^{4+} between stellar winds in the SMC and the Galaxy. Figure 9 underlines this conclusion. The marginally higher ionization fractions of C^{3+} and N^{4+} in the SMC stars could easily be compensated by adopting a somewhat higher value for the SMC metallicity. In fact, the value of Z(SMC) = 0.1 Z(MW) may be on the low side for what is usually assumed in the literature. We conclude that mass-loss rates in the SMC derived from Hα and from the UV agree within the observa-

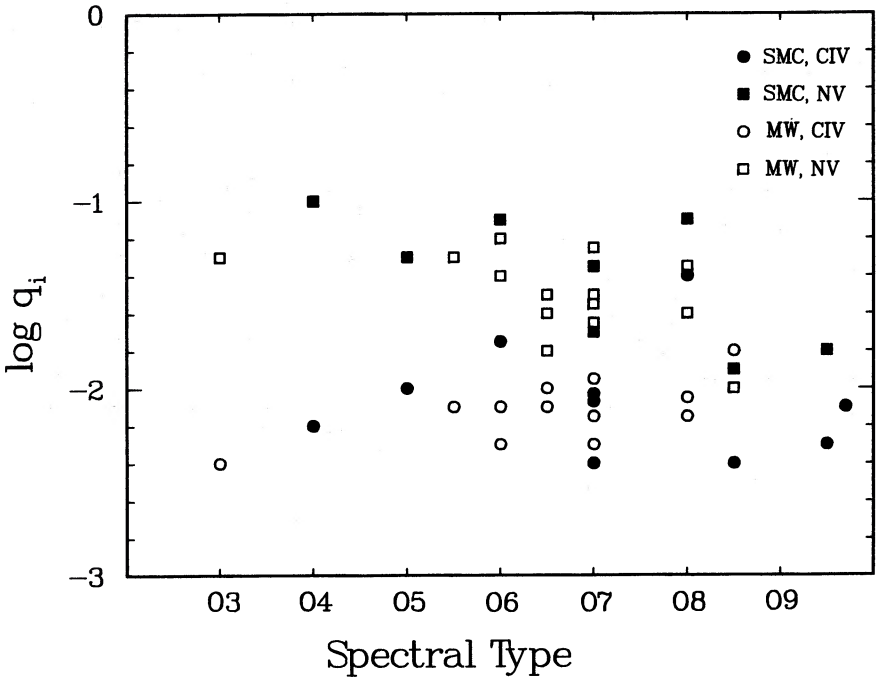

FIG. 9.—Derived ionization fractions of C^{3+} and N^{4+} vs. spectral type. The results for the SMC stars are compared with results found for galactic stars.

tional uncertainties if standard values for the ionization fractions and for the chemical abundances of SMC stars are adopted.

VII. CONCLUSIONS

Precise mass-loss rates for luminous extragalactic O stars are of crucial importance for our understanding of the photospheric conditions and the stellar evolution of very massive stars. In this paper we investigated the theoretical prediction by the radiation-pressure–driven wind theory of significantly lower mass-loss rates in metal-poor galaxies like the SMC and the LMC than in our Galaxy.

We studied the stellar-wind properties of a representative sample of 26 O stars in the SMC and LMC. To this end we used the Hα line which proves to be a reliable and observationally simple technique to derive mass-loss rates in extragalactic O stars. Since the Hα luminosity emitted by the wind does not depend on the chemical abundances and the ionization states of elements heavier than helium, whereas UV-$\dot{M}$ techniques do, a comparison of mass-loss rates derived by Hα and the UV allows us to constrain Z and q_i in O stars. Hα and UV data agree if the canonical abundances for the SMC and standard galactic ionization fractions are adopted for the UV.

Mass-loss rates predicted by the radiation-pressure–driven wind theory have been calculated from simple scaling relations. Our parameter study confirms the earlier result that on the average the theoretical mass-loss rates should scale with a factor $\sim(Z)^{1/2}$. However, the dependence of $\dot{M}_{\rm the}$ on the metallicity is rather weak as compared with dependences on other stellar parameters, especially on the stellar luminosity. Since the luminosity of O stars is controlled by the behavior of the energy distribution in the UV around 1000 Å, the theoretically predicted mass-loss rates are strongly affected by uncertainties in the adopted effective temperatures and bolometric corrections. Most of the scatter in the values for $\dot{M}_{\rm the} - \dot{M}_{\rm obs}$ for galactic stars shown in Figures 3 and 5 can be ascribed to this effect. We note that uncertainties in the adopted stellar parameters may also affect the observed $\dot{M}/L$ relations. In fact, much of the scatter around the observed $\dot{M}/L$ relations published by Garmany and Conti (1984) can be explained by random errors in the adopted luminosities. The scatter may not necessarily imply a dependence of $\dot{M}$ on other stellar parameters.

Observed and theoretical mass-loss rates in the Magellanic Clouds systematically disagree if the stellar parameters associated with an SMC/LMC star of a certain spectral type are assumed to be the same as those of a galactic star of identical spectral type. However, only small modifications of the assumed effective temperatures and luminosities have dramatic consequences on the theoretical mass-loss rates (with virtually no effect on the observed rates). We have shown that theory and observations agree if SMC stars have effective temperatures hotter by ~10% (and LMC stars by ~5%) than corresponding galactic O stars. Part of the disagreement between observed and theoretical values could also be removed by larger distance moduli for the Clouds than generally adopted. Especially in the SMC, however, the most plausible assumption to reconcile theory and observations is a hotter $T_{\rm eff}$ scale. In view of these uncertainties we are inclined to believe that the radiation-pressure–driven wind theory predicts the correct functional dependence of $\dot{M}$ on Z for the Magellanic Clouds. It seems implausible that the theory happens to predict correct mass-loss rates just for stars with galactic abundances. Photospheric analyses of O stars in the Clouds are needed to confirm or reject the assumption of effective temperatures systematically hotter in the Magellanic Clouds than in the Galaxy.

I especially appreciate numerous conversations with David Abbott on the theory of stellar winds. Thanks are due to Peter Conti and Katy Garmany for their encouraging interest and support for this project. This work has been supported by a Feodor-Lynen Fellowship of the Alexander-von-Humboldt Foundation and by NSF grant AST 85-20728 through the University of Colorado.

REFERENCES

Abbott, D. C. 1982, *Ap. J.*, **259**, 282.
———. 1985, in *Radio Stars*, ed. R. M. Hjellming and D. M. Gibson (Dordrecht: Reidel), p. 61.
Abbott, D. C., Bieging, J. H., Churchwell, E., and Torres, A. V. 1986, *Ap. J.*, **303**, 239.
Abbott, D. C. and Hummer, D. G. 1985, *Ap. J.*, **294**, 286.
Auer, L. J., and Mihalas, D. 1972, *Ap. J. Suppl.*, **24**, 193.
Azzopardi, M., and Breysacher, J. 1979, *Astr. Ap.*, **75**, 120.
Azzopardi, M., and Vigneau, J. 1982, *Astr. Ap. Suppl.*, **50**, 291.
Bruhweiler, F. C., Parsons, S. B., and Wray, J. D. 1982, *Ap. J.*, **256**, L49.
Brunish, W. M., and Truran, J. W. 1982, *Ap. J. Suppl.*, **49**, 447.
Castor, J. I., Abbott, D. C., and Klein, R. I. 1975, *Ap. J.*, **195**, 157 (CAK).
Chiosi, C., and Maeder, A. 1986, *Ann. Rev. Astr. Ap.*, **24**, 329.
Conti, P. S., Garmany, C. D., and Massey, P. 1986, *A.J.*, **92**, 48.
Friend, D. B., and Abbott, D. C. 1986, *Ap. J.*, **301**, 701 (FA).
Garmany, C. D., and Conti, P. S. 1984, *Ap. J.*, **284**, 705.
———. 1985, *Ap. J.*, **293**, 407.
Garmany, C. D., Conti, P. S., and Massey, P. 1987, *A.J.*, **93**, 1070.
Garmany, C. D., and Fitzpatrick, E. L. 1988, *Ap. J.*, **332**, 711.
Garmany, C. D., Olson, G. L., Conti, P. S., and Van Steenberg, M. E. 1981, *Ap. J.*, **250**, 660.
Garmany, C. D., and Walborn, N. R. 1987, *Pub. A.S.P.*, **99**, 240.
Humphreys, R. M. 1987, in *Instabilities in Luminous Early-Type Stars*, ed. H. Lamers and C. de Loore (Dordrecht: Reidel), p. 3.
Kudritzki, R. P., Pauldrach, A., and Puls, J. 1987, *Astr. Ap.*, **173**, 293 (KPP).
Lamers, H. J. G. L. M. 1988, in *Mass Loss in Astronomical Objects*, ed. L. Bianchi and M. Grewing (Dordrecht: Reidel), in press.
Leitherer, C. 1988, *Ap. J.*, **326**, 356 (Paper I).
Maeder, A., and Meynet, G. 1987, *Astr. Ap.*, **182**, 243.
Massey, P. 1985, *Pub. A.S.P.*, **97**, 5.
Pauldrach, A., Puls, J., and Kudritzki, R. P. 1986, *Astr. Ap.*, **164**, 86 (PPK).
Prinja, R. K. 1987, *M.N.R.A.S.*, **228**, 173.
Sanduleak, N. 1969, *Cerro Tololo Inter-American Obs. Contrib.*, No. 89.
Schmidt-Kaler, T. 1982*a*, in *Landolt-Bornstein, New Series, Group VI*, Vol. **26**, ed. K. Schaifers and H. H. Voigt (Berlin: Springer), p. 1.
———. 1982*b*, in *Landolt-Bornstein, New Series, Group VI*, ed. K. Schaifers and H. H. Voigt (Berlin: Springer), p. 449.
Shore, S. N., and Sanduleak, N. 1984, *Ap. J. Suppl.*, **55**, 1.
Walborn, N. R. 1986, in *IAU Symposium 116, Luminous Stars and Associations in Galaxies*, ed. C. de Loore, A. Willis, and P. Laskarides (Dordrecht: Reidel), p. 185.
Willis, A. J., Howarth, I. D., Nandy, K., and Morgan, D. H. 1986, in *IAU Symposium 116, Luminous Stars and Associations in Galaxies*, ed. C. de Loore, A. Willis, and P. Laskarides (Dordrecht: Reidel), p. 269.

CLAUS LEITHERER: Joint Institute for Laboratory Astrophysics, University of Colorado, Boulder, CO 80309-0440